ISES International Solar Energy Society

Conference Proceedings

EuroSun 2014

Aix-les-Bains (France), 16 – 19 September 2014

Performance Analysis of Uncovered PV-T Collectors for Radiative Cooling and Heating Applications

Xavier Jobard[1], Reiner Braun[1], Nansi Palla[2], Jan Cremers[2] and Ursula Eicker[1]

[1] Center for Sustainable Energy Technology/HFT-Stuttgart, Stuttgart (Germany)

[2] Center for Integral Architecture/HFT-Stuttgart, Stuttgart (Germany)

Abstract

New uncovered photovoltaic-thermal (PV-T) collectors were developed and tested to produce electricity, chilled and hot water. The use of uncovered PV-T collectors has already been investigated for heating applications. However uncovered PV-T collectors are also interesting for radiative cooling applications. This concept was already demonstrated in two plus energy houses that participated in the Solar Decathlon Europe competition. The working principle of radiative cooling is to use the radiative heat loss of the collector top surface to cool down a fluid which is then used to air-condition a building

This paper focuses on the collector design characteristics and their performances for radiative cooling and heating applications. The procedure for the performance characterization is inspired from the quasi dynamic test method for uncovered thermal collector of the new EN ISO 9806:2014. For the identification of the collector parameters GenOpt has been coupled with TRNSYS. These coefficients are then used to establish the thermal efficiency curves for heating and cooling applications: the results of three different PV-T collector designs are compared between each other and to the performance of an uncovered solar collector.

Key-words: photovoltaic-thermal collectors, hybrid collectors, solar heating, renewable cooling, efficiency curves.

1. Introduction

Radiative cooling technologies for building application have been investigated for many years. Its principle is based on long-wave radiation heat transfer that is driven by the surface temperature difference between two bodies. On clear summer nights the difference between the sky temperature and the ambient temperature can range between 20 and 30 K (Bliss, 1961). Consequently, roof areas can be cooled below the ambient air temperature on conditions that the radiative heat losses of the roof toward the sky are maximized and therefore can be used to cool down a building.

Nevertheless, roof areas are in many cases used for the production of electricity with photovoltaic (PV) collectors. This conflict can be resolved by a combination of the two functions - electricity and thermal energy production - into one module, called a photovoltaic-thermal (PV-T) collector or hybrid collector.

PV-T collectors were developed and installed in two low-energy demonstration buildings that participated inthe Solar Decathlon Europe competition: "home^{+}" in 2010 and "Ecolar" in 2012. Simulation results show that 43% of the cooling load (location Madrid) of home^{+} can be covered by these PV-T collectors with measured mean specific cooling powers between 40 and 65 W/m² depending on the temperature level (Eicker and Dalibard, 2011).

In addition to providing chilled water for air-conditioning, these PV-T collectors can be used during daytime to generate electrical power and support a domestic hot water system and or a low temperature heating system. Also, the PV-cells are cooled increasing the PV-cells efficiency. This way, valuable surface areas of the building envelope can be used two- or threefold. This new kind of collectors can play a major role on reducing the primary energy consumption of buildings.

According to the IEA SHC Task 35, PV-T collector systems can be distinguished in four different categories;

Selection and/or peer review under responsibility of EuroSun2014 Scientific Committee
doi:10.18086/eurosun.2014.16.10 Available at http://proceedings.ises.org

flat-plate air collectors, flat-plate liquid collectors, concentrating PV-T collectors and ventilated facade integrated PV-modules (Hansen and Sorensen, 2006). Depending on the application, water-based flat plate collectors can be grouped furthermore into unglazed and glazed (covered) collectors. Unglazed collectors are more suitable for night time radiative cooling and low temperature heating, while glazed collectors are more suitable for domestic hot water production and space heating. Glazed PV-T collectors have a reduced PV efficiency since the fluid temperature is higher because the top cover which reduces the long wave radiative heat transfer and convection losses. However, this leads to higher stagnation temperature and thus lower electrical efficiency since the efficiency of PV-cells decreases up to 0,5% per 1K temperature rise (Weller et al., 2009). To prevent the decrease of the PV-cells efficiency, the collector must be cooled down constantly by a fluid, which means that the system needs a consumer load to discharge the heat. The glass cover also induces higher optical losses.

Until now 27 manufactures have been identified within the market analysis to produce unglazed PV-T liquid collectors with or without thermal insulation and using different technical solutions. Some manufacturers produce also only an absorber that can be mounted on the back of a PV-Module as a retrofit. The producers of covered PV-T collectors are not so numerous; only 5 manufacturers could be identified.

The constructive aspects of PV-T collectors that have an impact on their thermal performance are mainly the thermal bond between the PV module and the thermal absorber and the thermal resistance of the PV module itself which are dependent of the design and the manufacturing possibilities.

There are different possibilities to connect these two parts: lamination, pressing and gluing for example. For high thermal performances, this connection should be ensured on the largest area possible, thus a direct lamination of the PV module on the absorber seems to be the best options till now. The contact area is then maximized and the thermal resistance of the bond is minimized since lamination requires no additional material. However this technic is not yet a standard, mainly because of the lack of suitable materials with the right properties and lack of experience on this field. One of the most critical properties is the thermal expansion coefficient of the PV module and thermal absorber. If the dilatation of the different material used are too different, inflexible joining technics such as gluing and lamination causes mechanical stress on the bond leading to its destruction when the collector experience big temperature variation. Consequently, the connection has to be flexible enough to balance the upcoming dilatation of the chosen materials in addition to a small thermal resistance. Besides the thermal performance there are other important aspects such as costs, durability and recyclability that go along with a new collector design.

Furthermore the building integration of uncovered collectors also has a considerable impact on the performance e.g. the better the view factor to sky is, the better the thermal performances for night radiative cooling are. Backside insulation or an air gap between the module and the roof/wall are further aspects, depending on the application these constructive issues are convenient for low temperature heating and radiative cooling systems. The electrical performance depends on the same aspects as for simple PV modules with the potential to increase the output through the cooling of the module during daytimes.

This paper focuses on the performance characterization of such collectors and the comparison of four different designs. First, the different PV-T collector designs will be presented, and then the means and method of the experimental set up. Finally the tests results will be presented and discussed.

2. Design Characteristics of PV-T collectors for radiative cooling applications

Uncovered flat plate collectors seem to be a pertinent collector design for radiative cooling applications since they offer large areas oriented to the sky while the top cover of glazed/covered collectors reduces the radiative heat transfer coefficient of the absorber. However the performances of such collectors for heating are very low at higher temperature levels. The heat transfer medium can be either water or air based. Water based systems seem to offer more advantageous, since the piping is more compact making building integration easier, and the heat capacity of the fluid is higher thus reduces the amount of work needed to pump the fluid.

There are many possibilities of PV cells and absorber combinations: these go from laminated PV modules with crystalline silicon cells to thin film modules, both in combination with normal absorber plates with harp or serpentine piping to holohedral plastic or metal absorbers. The presented collectors within this paper are only constructed with a holohedral polypropylene absorber. Because of the high difference between the dilatation coefficient of the polypropylene absorber and the PV modules used, the connection techniques of all these

presented prototypes are pressed or clamped on the back side of a silicon PV module.

Fig.1 presents the four collector's designs under investigation:

- Collector A is an uncovered polypropylene holohedral thermal absorber without PV, this collector is used as a reference collector for the comparison with collector type B, C and D,
- Collector B uses the same polypropylene absorber and a glass-PVB laminated PV module, both are pressed together within the frame,
- Collector C is of similar design as Collector B with the difference that between the absorber and the PV-module is an air gap,
- Collector D is composed of a glass-glass laminated PV module and the polypropylene absorber pressed together with aluminum U-profiles in diagonal, providing more contact zones. This collector was designed and implemented in the "Ecolar" building (HTWG, 2012). Fig. 2 presents the back side of Collector D.

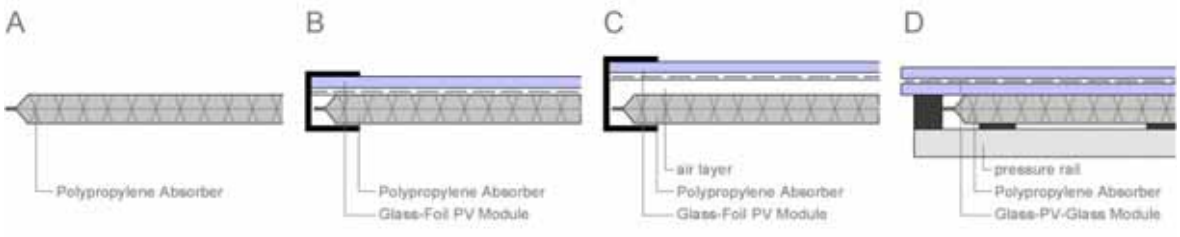

Fig. 1: Design Scheme of the investigated PV-T collectors A-D

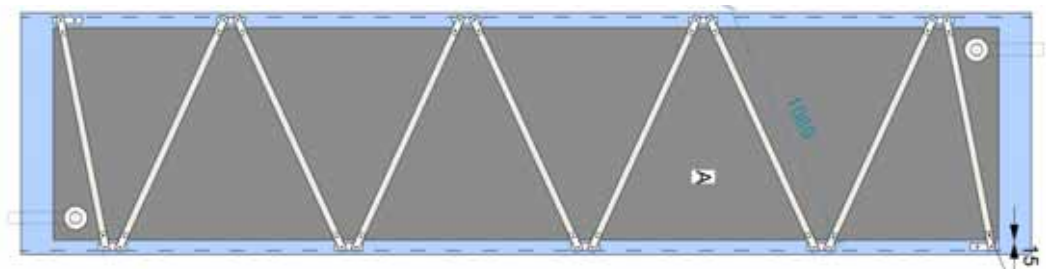

Fig. 2: Bottom view of Collector D (HTWG, 2012)

3. Test stand presentation

In order to measure the performance of the different investigated PV-T designs, an outdoor test stand was built on which up to five PV-T collectors can be tested simultaneously under dynamic conditions. Besides the obvious time gain, the main advantage of testing several collectors at the same time is that a direct comparison of the collector's performances is possible.

The thermal power output of the collectors is calculated from the measured volumetric flow rate and the temperature difference between the inlet and outlet of the collector. The wind speed and the global irradiation are measured in the collector plan. Finally the horizontal diffuse radiation is also collected. Fig. 3 presents views of the test stand and the inclination possibilities. The inlet temperature is controlled by the mean of a reversible chiller capable of maintaining the set temperature within ± 0.2 K. This device has also the capabilities to regulate the inlet temperature according to the ambient temperature.

Fig. 3: Views of the PV-T characterization test stand

Tab. 1 presents the instrumentation and their measurement uncertainty. The temperature sensors are PT100 with

a standard uncertainty at 20°C of 0.2 °C. The flow meters are magnetic inductive sensors with a standard uncertainty of 1% of the measured value. Cup anemometers were used, with an associated standard uncertainty of 0.3 m/s. The pyranometer used to measure the global solar irradiance in the collector plan have an expanded uncertainty of 1%. The horizontal diffuse radiation is measured with a shaded pyranometer, with an expanded uncertainty of 1.4%. The long wave irradiance is measured with a pyrgeometer with an expanded uncertainty of 4.5%. All the measurements are logged every 10s using an Ahlborn Almemo 5590-2 data logger and LabVIEW.

Tab. 1: Description, range and uncertainties of the installed instrumentation

Measured value	Sensor	Range	Uncertainty
Fluid temperature	Pt100 1/3 class B	-	0,1+0,005xT
Volumetric Flow	Magnetic inductive flow sensor SIKA VMZ	0.25 – 5 l/min	± 1%
Global Solar Irradiance	Pyranometer Huskeflux SR20	-	± 1%
Diffuse Solar Irradiance	Pyranometer Kipp&Zonen CMP21		± 1.4%
Wind speed	Cup Anemometer	0 – 10 m/s	±0.3 m/s
Long wave irradiance	Pyrgeometer Huskeflux IR20	-	4.5%

Fig. 4 presents the hydraulic scheme of the test stand and shows the location of the sensors.

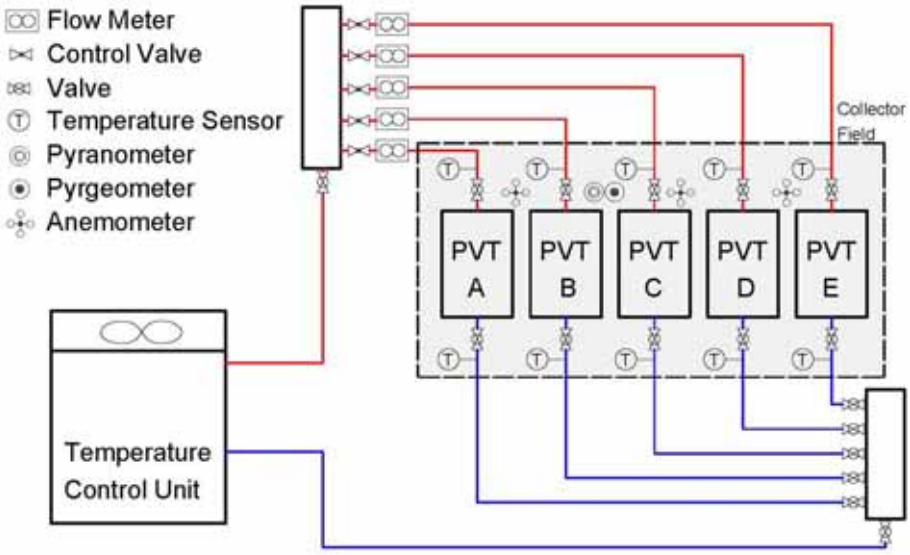

Fig.4: Hydraulic schema of the PVT test stand

4. Test period and procedure for the collector parameter identification

In June 2014 the new International Standard EN ISO 9806:2013: “Solar energy. Solar thermal collectors. Test methods” was published. This standard cancels and replaces the editions EN 12975-2:2006, ISO 9806-1:1994, ISO 9806-2:1995, and ISO 9806-3:1995, which have been technically revised. This international standard includes test methods for the thermal performance characterization of fluid heating collectors and it is also applicable to hybrid collectors. The test stand presented in the previous chapter is an outdoor test stand, therefore the procedure for the collector performance test is inspired form the quasi dynamic method (QDT) presented in the International Standard EN ISO 9806:2013.

4.1 PVT collector model

Type 203, developed at the Institute for Solar Energy Research Hameln (ISFH) (Stegmann and Bertram, 2011, Bertram and Stegmann, 2011), simulates an unglazed photovoltaic-thermal collector not only for heat and electricity production but also for the radiative cooling application. The energy balance for the thermal part of the PV-T collector model of type 203 is given by eq. 1. The electrical part is modelled according to the EN

60904 and the thermal part according the EN 12975. Different calculation modes are available depending on the number of known parameter and inputs.

$$c_{eff}\frac{dT_m}{dt} = \dot{q}_N - E_n^*\eta_0(1 - b_u u) + (b_1 + b_2 u)(T_m - T_a) \quad \text{(eq. 1)}$$

Where:

- c_{eff} (kJ/m^2 K) is the effective collector heat capacity,
- T_m and T_a (°C) are the mean fluid temperature and the ambient temperature,
- E_n^* (W/m^2) is the net incident angle-corrected irradiance given by :

$$E_n^* = E_n\left(k_b(\theta)\left(1 - \frac{G_d}{G_g}\right) + k_d\frac{G_d}{G_g}\right) \quad \text{(eq. 2)}$$

  With k_b the incident angle modifier (IAM) coefficient for beam radiation, k_d the IAM coefficient for diffuse radiation, G_g and G_d are respectively the global and diffuse solar irradiance. E_n is the net irradiance and is given in equation eq. 3,

$$E_n = G_g + \left(\frac{\varepsilon}{\alpha}\right)_{abs}\sigma\left(T_{sky}^4 - T_a^4\right) \quad \text{(eq. 3)}$$

- η_0 (-) is the conversion factor,
- u (m/s) is the wind velocity,
- b_u (s/m) is the wind dependence factor for η_0,
- b_1 (W/m^2 K) is the heat loss coefficient,
- b_2 (J/m^3 K) is the wind dependence factor for b_1,
- $\dot{q}_N$ (W/m^2) is the specific thermal collector output power and can also be written as a function of the fluid mass flow $\dot{m}$ (kg/s), specific heat capacity c (J/kg K), inlet and outlet temperature T_i and T_o (°C) and the gross collector aperture A (m²) is given by:

$$\dot{q}_N = \frac{\dot{m}\, c\, (T_o - T_i)}{A} \quad \text{(eq. 4)}$$

4.2 Test period

The temperature control unit at the test stand (see Fig. 4) has the possibility to control the inlet temperature as a function of the ambient temperature in the range of ±30 °C. For the collector parameter identification three days with different fluid inlet temperatures where used (a) inlet temperature closed to ambient temperature, (b) inlet temperature = ambient temperature + 7 °C and, (c) inlet temperature = ambient temperature + 15 °C.

Fig. 5 shows the measured weather conditions for the ambient and sky temperature and the global radiation for the three days. The figure shows that the global radiation has been fluctuating during the test period. Fischer et al. (2004) compared the steady-state testing method to the quasi-dynamic method, the major difference is that the test data for the quasi-dynamic method can be collected during the whole day. He showed that for days with variable irradiance the time period between 9 am and 4 pm can be used for the analysis. The mean, minimum, maximum and the standard deviation of the weather conditions and the temperature difference during the test period are listed in table 2. The measured data represents a useful range of measured data for this kind of collectors for the analysis.

The typical range for the difference between the average fluid temperature and the ambient temperature (T_m - T_a) for uncovered and uninsulated collectors can reach 20 - 25 K. Therefore the whole range of the temperature difference should be represented in the data.

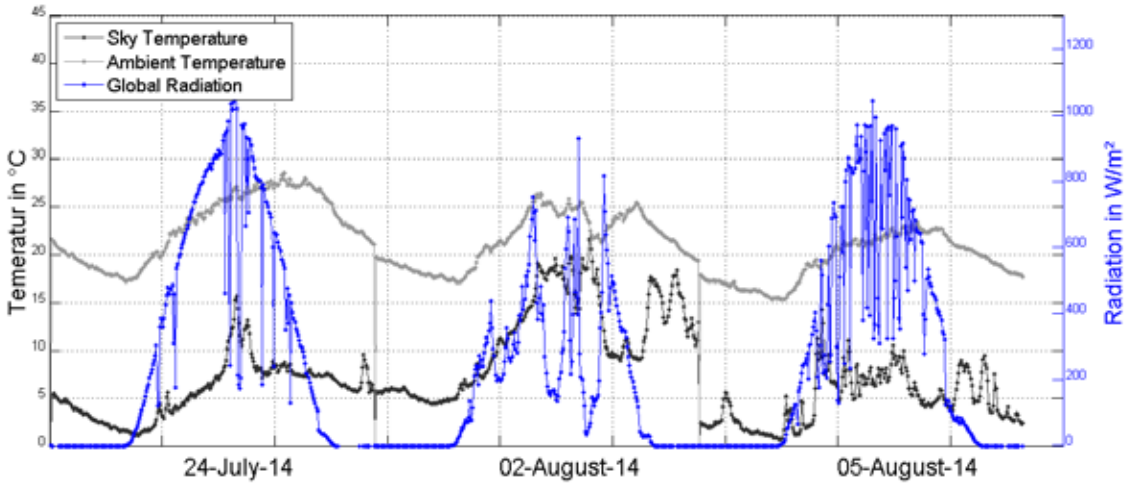

Fig. 5: Measured ambient temperature, sky temperature and the global radiation for the three test days

Tab. 2: Conditions during the measurement phase

Weather station data				
	Mean	**Min.**	**Max.**	**Standard deviation**
Ambient temperature in °C	23,9	20,6	27,6	1,93
Wind speed in m/s	1,16	0,07	5,03	0,78
Radiation in W/m²	593	41	1061	277
Sky temperature in °C	10,8	4,7	21,7	4,8
PVT test stand data				
(Tm – Ta) in °C for collector type A	8,6	0,7	17,1	5,6
(Tm – Ta) in °C for collector type B	7,9	0,6	15,9	5,7
(Tm – Ta) in °C for collector type C	7,7	0,7	15,6	5,5
(Tm – Ta) in °C for collector type D	8,1	0,7	16,2	5,7

4.3 Collector parameter identification process

For the identification of the collector parameters the Multi-Start GPS Algorithm (GPSHookeJeeves), has been implemented in GenOpt and coupled with TRNSYS. Therefore the output of the fluid outlet temperature from TRNSYS collector model Type 203 was fitted against the measured data. The aim was to find a parameter set which has the lowest deviation between the modelled and simulated output (eq. 5).

$$L = \sum_{i=1}^{n} (T_{os,i} - T_{o,i})^2 \qquad \text{(eq. 5)}$$

With :

- L is the sum of squared errors of the temperature difference
- $T_{os,i}$ is the simulated fluid outlet temperature
- $T_{o,i}$ is the measured fluid outlet temperature

Fig. 6 shows the comparison between measured and simulated power output for the different collectors. For this comparison the whole data set (day and night) was considered, the negative values represent the night data where the fluid was cooled down. Tab. 3 shows the mean values and the standard deviation for the temperature difference and the collector power output between the calculated values from the model and the measurement. Collector A and C have the lowest difference between modeled and measured values. The results for collector B have the highest difference of all collectors, especially at night time where the collector is producing chilled water. Table 4 summarizes the calculated collector parameters, as expected has collector A the highest efficiency from all collectors. Collector C with the air gap between the PV module and the thermal collector has the lowest efficiency.

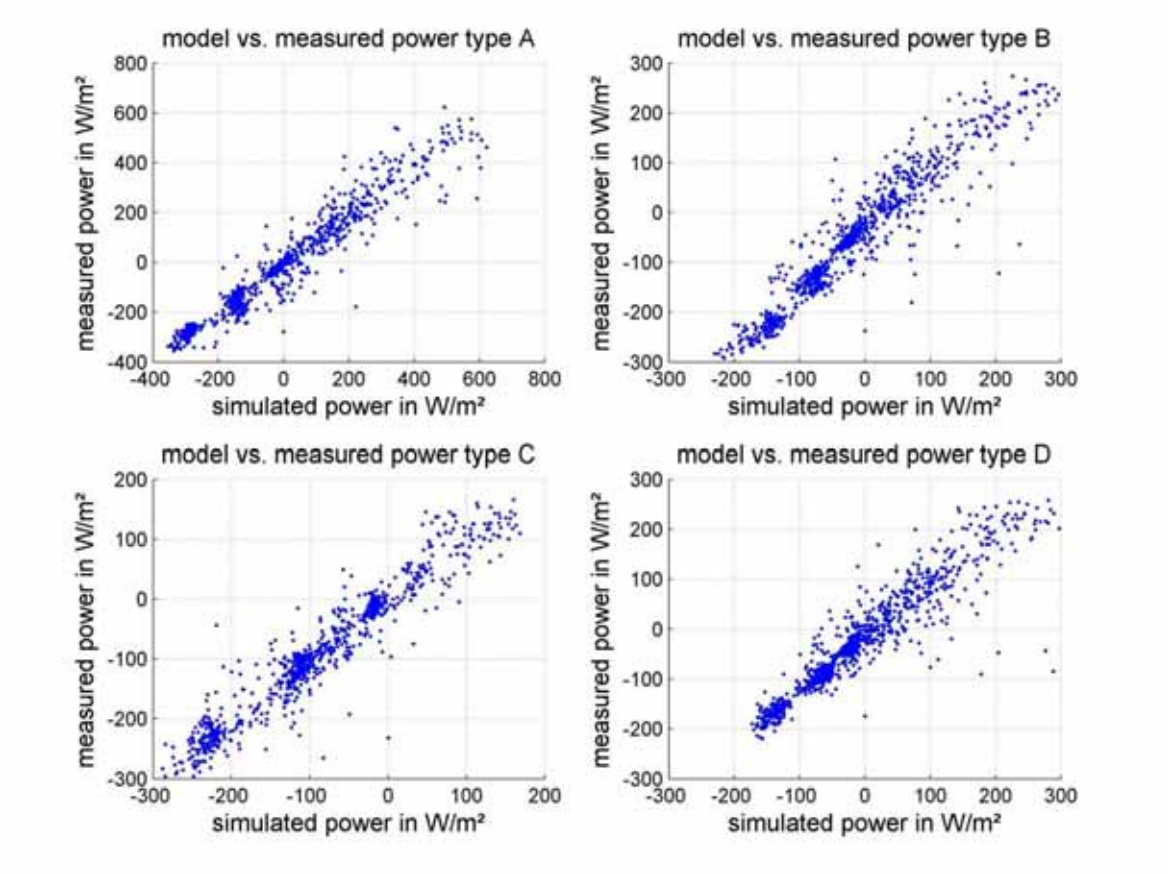

Fig. 6: Comparison between measured and simulated power output for all four collector types

Tab. 3: Standard deviation between the modelled and measured data for the return temperature and power output of the collectors

	mean values for dT	Standard deviation for dT	mean values for dQ	Standard deviation for dQ
Collector type A	0,06	0,41	9,9	57,6
Collector type B	0,24	0,30	35,6	41,6
Collector type C	0,01	0,19	2,2	28,9
Collector type D	0,11	0,24	16,5	33,3

Tab. 4: (Simulation) Identified Parameter for the analysed PVT modules

	Type A	Type B	Type C	Type D	Units
Conversion factor $\boldsymbol{\eta_0}$	0,81	0,43	0,25	0,38	[-]
Collector heat loss coefficient $\boldsymbol{b_1}$	18,1	7,23	15,17	7,67	[W/m^2 K]
$\boldsymbol{b_1}$ wind dependence factor $\boldsymbol{b_2}$	5,18	7,06	4,87	2,86	[J/m^3 K]
$\boldsymbol{\eta_0}$ wind dependence factor $\boldsymbol{b_u}$	0,017	0,014	0,005	0,008	[s/m]
Effective collector heat capacity $\boldsymbol{c_{eff}}$	26	41	24	38	[kJ/m^2 K]
Emmitance aborptance ratio $(\boldsymbol{\varepsilon/\alpha})_{\boldsymbol{abs}}$	0,52	0,99	0,89	0,99	[-]

5. Results and discussion

4.4 Efficiency curves for heating application

In order to compare the different collectors between each other, the efficiency of the collectors needs to be established over a wide range of weather conditions and applications. One of the most efficient method is to plot the thermal efficiencies of the different collectors versus the temperature difference between the mean fluid temperature T_m and the ambient temperature T_a for a given solar irradiance, wind velocity, sky and ambient

temperature. By assuming steady state conditions, the collector heat flux can be derived from equation eq. 1 and is given in eq. 6.

$$\dot{q}_N = E_n^* \, \eta_0(1 - b_u u) - (b_1 + b_2 u)(T_m - T_a) \quad \text{(eq.6)}$$

For normal beam radiation, the incidence angle modifier is equal to 1, E_n^* is then equal to the net irradiance E_n given in eq. 3, if the IAM coefficient for diffuse radiation is neglected. Finally the efficiency is expressed as the ratio of the heat flux over the global solar irradiance:

$$\eta_H = \frac{\dot{q}_N}{G_g} \quad \text{(eq.7)}$$

Fig. 7 shows the efficiency curves for the four collectors for a global solar irradiance at different global solar irradiance (800W/m² on the left and 300 W/m² on the right). The wind velocity, the ambient temperature and the sky temperature are constant and respectively equal to 2 m/s, 20°C and 5°C. Because Collector A has the lowest thermal resistance between the front surface and the fluid (no PV-module), it performs the best over the whole range of temperature difference and for both irradiance. Compared to the other collectors, collector D obtains a lower slope than the other collectors which can be explain by the fact that the backside of the absorber is mostly shielded from the wind and because of a higher thermal resistance of the PVT module induces by its glass-glass construction.

Every PV-T modules (B C and D) show a lower efficiency when the temperature difference is equal to zero, which means that the bonding between the PV module and the polypropylene absorber is crucial, in order to obtain a thermally efficient PV-T collector.

For under ambient temperature applications, none of the PV-T collectors has a better efficiency than collector A and they seem to be performing identically passed a certain temperature difference. The air gap of Collector C is a clear disadvantage when the solar irradiance is important. However as shown in Fig. 7 left, for low solar irradiance the performance difference is less important, but the heat flux output of such collector at low irradiance is small.

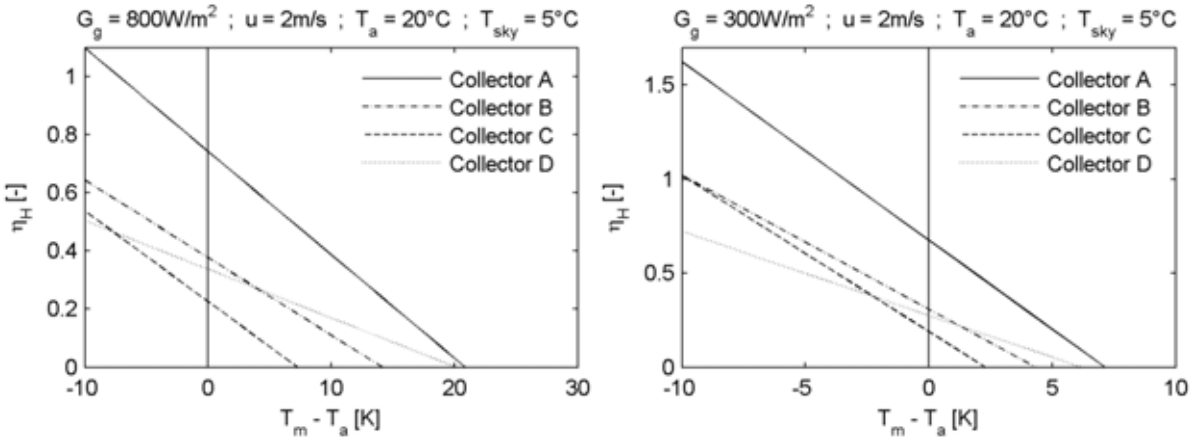

Fig. 7: Efficiency Curves for heating application at different weather conditions.

4.4 Efficiency curve for radiative cooling application

In the same way as previously, the efficiency curve for radiative cooling application can derived for equation eq. 1. In this case the heat flux is expressed the same way as in equation eq. 6. The net irradiance E_n^* is derived from equation eq.3, however since the global radiation is zero, E_n is equal to the net long wave irradiance $E_{n,l}$ expressed as the factor of the long wave irradiance E_l given in eq. 7 and emittance and absorptance ratio $(\varepsilon/\alpha)_{abs}$ of the absorber :

$$E_l = \sigma\left(T_{sky}^4 - T_a^4\right) \quad \text{(eq. 7)}$$

$$E_{n,l} = \left(\frac{\varepsilon}{\alpha}\right)_{abs} E_l \quad \text{(eq. 8)}$$

As the net long wave radiation is the maximum available resource for nighttime cooling application, the efficiency in this case is expressed as followed:

$$\eta_C = \frac{\dot{q}_N}{E_l} \qquad \text{(eq. 9)}$$

Fig. 8 shows the efficiency curves for cooling application for constant wind velocity, ambient temperature and sky temperature respectively equal to 2 m/s, 20°C and 5°C. In contrast to the heating application, efficiency curves for cooling application increases with the temperature difference between the mean fluid temperature and the ambient temperature.

The efficiencies of collectors A, B and D are similar for a temperature difference close to zero. According to this result two factors are important for radiative cooling the absorber/PV-module bonding and the emittance absorptance ratio of the collector. Collector A has the lowest thermal resistance between fluid and the ambient, however its emittance absorptance ratio is lower compared to the PV-T modules B and D. That could explain the close value of these collector's efficiencies at $T_m - T_a$ equal to zero. Collector C does not perform as well as the other for low and negative temperature differences because of the air gap between the absorber and the PV module which reduces the radiative heat loses toward the sky of the collectors. However, as the temperature difference increases, the convective part of the heat loses grows and the efficiency of collector C is closer to the efficiencies of collector A and B and higher than the efficiency of collector C. As for heating application, the small slope of collector C is explained by the wind dependency coefficient of the heat loss coefficient (b_2) which is lower compared to the order collectors as shown in Tab. 4.

Finally this figure shows that cooling a fluid under the ambient temperature leads to low efficiency: All of the collectors have efficiencies lower than 0.5 as well as low heat fluxes. A these ambient and sky temperatures, the long wave irradiance is -79 W/m² resulting in heat fluxes lower than -40 W/m².

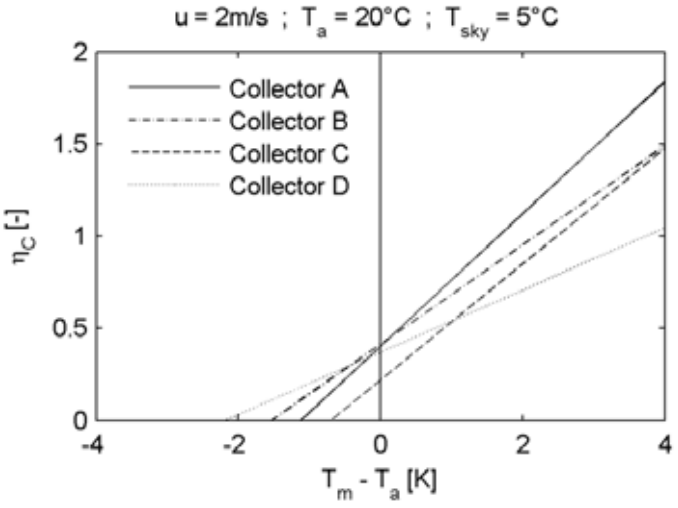

Fig. 8: Efficiency Curves for radiative cooling application at different weather conditions

6. Conclusion

The thermal performances of three different uncovered PV-T collectors were investigated for heating and radiative cooling applications and compared to an uncovered solar collector (collector A). All collectors uses the same holohedral polypropylene absorber, the bonding technic between the absorber and the PV module is however different. The experimental measurements at the outdoor test stand were performed under dynamic conditions. The measurements were then used to identify the collector parameters of the PV-T TRNSYS model type 203. The efficiency curves of the collector were then established using these parameters. Good matches between the modeled and measured data were obtained for the collectors A, C and D. Collector B has the highest difference from the measurement, expecially at night time. The comparison of the efficiencies shows that for heating applications with uncovered PV-T collectors the bonding between the absorber and the PV module is crucial. However for radiative cooling, two factors are important first the absorber PV-module bonding and second the emittance absorption ratio of the collector.

Acknowledgements

The project PVTintegral is funded by the German Federal Ministry of Education and Research (BMBF). Support code: 03FH029I2.

Partners: MEFA Energy Systems / Isosol UG / Watts Industries Deutschland GmbH / ertex solartechnik GmbH / Solarzentrum Allgäu GmbH & Co. KG

The project PVT HeatCool is funded by the Ministry of Science, Research and the Arts of the State of Baden-Wuerttemberg and European Regional Development Fund (EFRE). Support code: 32-7532.40/44.

Partners: Universität Stuttgart ITW / HTWG Konstanz /

MEFA Energy Systems / Transsolar Energietechnik GmbH

Paragraph 1, 2, 3 and 5 comes from the PVTIntegral project
Paragraph 3, 4 and 5 comes from the HeatCool project

References

Bertram, E., Stegmann, M., 2011. Heat pump systems with borehole heat exchanger and unglazed PVT-collector. ISES – Solar World Congress.

Bliss, R., 1961. Atmospheric radiation near the surface of the ground: a summary for engineers. Solar Energy 5, 103–120.

Eicker U., Dalibard A., 2011. Photovoltaic–thermal collectors for night radiative cooling of buildings. Solar Energy. 85, 1322-1335.

Fischer, S., Heidemann, W., Mueller-Steinhagen, H., Perers, B., Bergquist, P., Hellstro¨m, B., 2004. Collector test method under quasi-dynamic conditions according to the European Standard EN 12975–2. Sol. Energy 76 (1–3), 117–123.

Hansen, J. and Sorensen, H., 2006. Paper on Task 35 and PV/Thermal Solar Systems from the World Renewable Energy Congress on August 19-25, 2006 in Firenze, Italy. Document Number: DE2-3.

HTWG Konstanz, University of Applied Sciences, 2012. Contribution to Solar Decathlon Europe 2012, www.ecolar.de.

Stegmann, M., Bertram, E., 2011. Model of an unglazed photovoltaic thermal collector based on standard test procedures. ISES – Solar World Congress.

Weller, B., Hemmerle, C., Jakubetz, S., Unnewehr, S., 2009. Photovoltaik. Technik Gestaltung Konstruktion. München: Detail, p. 23.